Giordano, Lorenzo; Derikvand, Mohammad; Fink, Gerhard

Bending Properties and Vibration Characteristics of Dowel-Laminated Timber Panels Made with Short Salvaged Timber Elements

Published in:
Buildings

DOI:
10.3390/buildings13010199

Published: 11/01/2023

Document Version
Publisher's PDF, also known as Version of record

buildings

MDPI

Article

Bending Properties and Vibration Characteristics of Dowel-Laminated Timber Panels Made with Short Salvaged Timber Elements

Lorenzo Giordano, Mohammad Derikvand * and Gerhard Fink

Department of Civil Engineering, Aalto University, 02150 Espoo, Finland
* Correspondence: mohammad.derikvand@aalto.fi

Abstract: Salvaged timber elements often have length limitations, and therefore, their reuse in structural products normally would require additional processing and end-to-end joining. This increases the costs of reusing such materials, which makes them even less attractive to the timber sector. In the presented research, a new approach is proposed for reusing short, salvaged timber elements combined with new (full-scale) timber boards to fabricate dowel-laminated timber (DLT) panels without significant processing or end-to-end joining or gluing. In this approach, salvaged timber elements are pressed in the system in such a way that they can contribute to the bending performance of the DLT panels by resisting compression stress. In order to evaluate the effectiveness, several small-scale and large-scale DLT panels were fabricated. Salvaged plywood tenons were used as connectors. The bending stiffness of the small-scale DLT panels and the first eigenfrequency, damping ratio, bending properties, and failure modes of the large-scale DLT panels were evaluated. The results exhibited that by using the proposed approach, the short, salvaged timber elements can contribute substantially to the bending stiffness of the DLT panels without requiring end-to-end joining or gluing. On average, about a 40% increase in the bending stiffness could be achieved by pressing in the salvaged timber elements, which results in relatively similar stiffness properties compared to conventional DLT panels. One further characteristic is that the failure of the panels, and therefore the panel's strength, is mainly governed by the quality of the full-scale timber boards instead of the salvaged ones. This can be beneficial for practical use as the qualitative assessment of the strength properties of salvaged timber becomes less critical.

Keywords: dowel-laminated timber; bending stiffness; eigenfrequency; damping ratio; salvaged plywood; wooden connectors; reuse; circular economy

Citation: Giordano, L.; Derikvand, M.; Fink, G. Bending Properties and Vibration Characteristics of Dowel-Laminated Timber Panels Made with Short Salvaged Timber Elements. *Buildings* **2023**, *13*, 199. https://doi.org/10.3390/buildings13010199

Academic Editor: Andreas Ringhofer

Received: 28 November 2022
Revised: 27 December 2022
Accepted: 10 January 2023
Published: 11 January 2023

1. Introduction

Due to increased demands toward a circular economy, reusing salvaged timber materials in new applications has received specific research attention in recent years [1–5]. Salvaged timber can come from a variety of sources, such as demolished buildings, construction sites, timber production facilities, or even dead standing trees. Therefore, a large quantity of salvaged timber is created in different sectors every year, which has the potential to become marketable for certain applications. Currently, some well-established approaches exist involving the case of 'recycling' of salvaged timber, e.g., by turning them into wood particles to produce particleboard (see, e.g., [6,7]). For recycled timber in, e.g., Australia, even an interim industry standard is available (see [8–10] for further information). Nevertheless, the direct use of salvaged timber materials in their solid form without requiring significant processing is still limited. In this regard, reusing salvaged timber in fabricating structural mass-laminated timber products has been explored in a few studies. Llana et al. [11], for example, obtained salvaged European oak timber (*Quercus robur* L.) from the demolition of a 200-year-old building and utilized it for fabricating cross-laminated timber (CLT). In another research, Ma et al. [12] investigated the effectiveness of using

salvaged timber obtained from dead standing white spruce trees (*Picea glauca*) for CLT fabrication. Arbelaez et al. [13] investigated the mechanical properties of 3-layer CLT panels fabricated with varying amounts of salvaged timber in different layups. Rose et al. [14] utilized salvaged timber obtained from both construction sites and demolition sites as a feedstock for fabricating so-called cross-laminated secondary timber. In all those studies, efficient mechanical properties were reported.

The above research works have demonstrated the feasibility of reusing salvaged timber in fabricating mass-laminated timber products; however, there are challenges that limit the widespread reuse of such materials. For example, most often, length limitation is one of the important challenges of reusing salvaged timber. Currently, the use of short timber elements in mass laminated timber is possible in general through finger jointing or other forms of end-to-end joining, e.g., [15,16]. These methods require processing the cross-section of the short timber elements and then gluing them together to create a longer board. However, the additional processing and the use of synthetic glues can affect the sustainability aspects and increase the cost of reusing salvaged timber elements.

In addition to length limitation, quantification of the mechanical properties is an important challenge. The mechanical properties of salvaged timber elements might be affected by natural aging phenomena, the duration of load effects (DOL, static fatigue, see, e.g., [17]), or mechanical and biological damages. The aging phenomenon is discussed by Cavalli et al. [18] based on a comprehensive literature review. Due to the large natural variability of the mechanical properties of timber [19,20] and the DOL effect, the quantification of the aging phenomena is difficult, and therefore, the results of the studies on the subject vary largely. Nevertheless, the original strength class, the load history, the environmental exposure, and the transport and storage conditions of salvaged timber might be unknown. In this case, a sufficient assessment is needed (see, e.g., [21,22] for assessment methods and approaches).

In the herein presented research, a new approach was investigated for reusing short, salvaged timber elements in fabricating dowel-laminated timber (DLT) panels without excessive processing or end-to-end joining or gluing. In practice, DLT products are normally fabricated with new (full-scale) timber boards using wooden dowels see [23,24]. In the proposed approach, however, salvaged timber elements were used in combination with full-scale timber boards to fabricate DLT panels. Salvaged plywood tenons were used as the connectors. The salvaged timber elements were pressed in the DLT panels in a way that they can contribute to the bending performance mostly by resisting compression stress in the system. Initially, the effectiveness of this approach was experimentally evaluated on small-scale DLT panels comprised of two layers of full-scale timber boards and one layer of salvaged timber elements. Afterward, a group of large-scale DLT panels was fabricated with three layers of full-scale timber boards and two layers of salvaged timber elements. The bending stiffness of the small-scale DLT panels and the first eigenfrequency, the damping ratio, and the bending stiffness of the large-scale DLT panels were evaluated both before and after pressing the salvaged timber elements in the system. Furthermore, the load-carrying capacity and the failure modes of the pressed-in large-scale DLT panels were investigated. The test results are summarized and discussed in this paper.

The main novelty of the research presented here lies in developing an alternative approach for mass laminated timber elements that are fabricated, in parts, with salvaged timber materials without significant processing or end-to-end joining. One specific characteristic of this approach is that the bending failure of the panels, and therefore their bending strength, is mainly governed by the quality of the full-scale timber boards rather than the salvaged timber. This is due to the fact that there is no end-to-end joining between the salvaged timber elements, which can be beneficial for practical use as the qualitative assessment of the strength properties of salvaged timber becomes less critical. Reducing the amount of processing and assessment needed to use salvaged timber can make such resources more profitable and, therefore, more attractive to the timber sector. This further

promotes the application of eco-friendly materials in the built environment and contributes to achieving the circular economy goals.

2. Materials and Methods

2.1. Materials

Sawn spruce timber boards (*Picea abies*) with the strength class C24 (assigned by the producer) and dimensions of width (w) × thickness (t) × length (l) = 117 × 44 × 3500 mm^3 were used as the full-scale timber boards in this study. They had no visible cracks but had some noticeable distortions because they had been stored in the laboratory environment with varying relative humidity for nearly two years prior to this research.

The salvaged timber elements were also spruce (*Picea abies*) with the original strength class C24 (initially assigned by the producer prior to their first use). They were recovered from several nail-laminated timber elements that had been destructively tested in another project [25,26]. The salvaged timber elements contained wooden nails and some cracks and wears from the previous application. They were also noticeably twisted and had other forms of shape irregularities as well. After minimal processing, the cross-sectional area of the salvaged timber elements was $w \times t$ = 117 × 44 mm^2, with the final length varying from 400 mm to 583 mm.

Salvaged birch plywood (19-mm-thick) was used for fabricating the tenon connectors. The use of plywood as a connector in different composite structures has also been the subject of a few previous studies [3,27,28]. In the study presented here, the salvaged plywood was obtained from the laboratory of the Civil Engineering Department at Aalto University. The salvaged plywood had been used as concrete formworks in other projects [29,30] prior to being utilized in this study.

2.2. Specimens

2.2.1. Small-Scale DLT Panels

The small-scale DLT panels were composed of two layers of full-scale timber boards and one layer of salvaged timber elements in the middle that were laminated together using the salvaged plywood tenons. The cross-sectional area of the salvaged plywood tenons was 38 × 19 mm^2 with l = 132 mm. The plywood tenons had rounded edges, as shown in Figure 1. The fabrication process, size, and minimum spacing of the salvaged plywood tenons were based on Derikvand et al. [3]. The middle layer of the small-scale DLT panels was made of three short, salvaged timber elements with the dimensions shown in Figure 1. The inner cross sections of the salvaged timber elements had been cut at an 88° angle (the inclination was selected within a trial-and-error process during the prototyping). The final dimensions of the small-scale DLT panels were breadth (b) × height (h) × length (l) = 132 × 117 × 1260 mm^3.

In total, eight small-scale DLT panels were fabricated and tested. In five panels, the cross sections of the salvaged timber elements in the center were profiled to create a tenon (see Figure 2). A mortise with similar dimensions was also cut on the cross-section of the adjacent salvaged timber elements. The mortise-and-tenon system was created in order to provide some form of end-to-end interlocking. It was assumed that the end-to-end interlocking system might potentially make the lamination process easier. However, three small-scale DLT panels were also fabricated without any end-to-end interlocking system to have a basis for comparison (Figure 2).

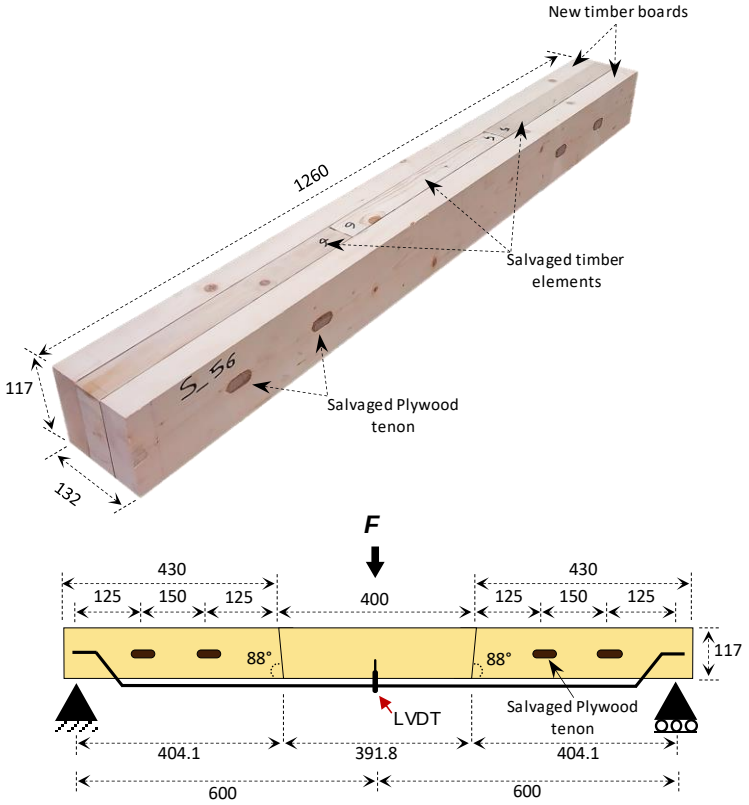

Figure 1. The dimensions of the salvaged timber elements in the small-scale DLT panels and the three-point bending test set-up. Dimensions in mm.

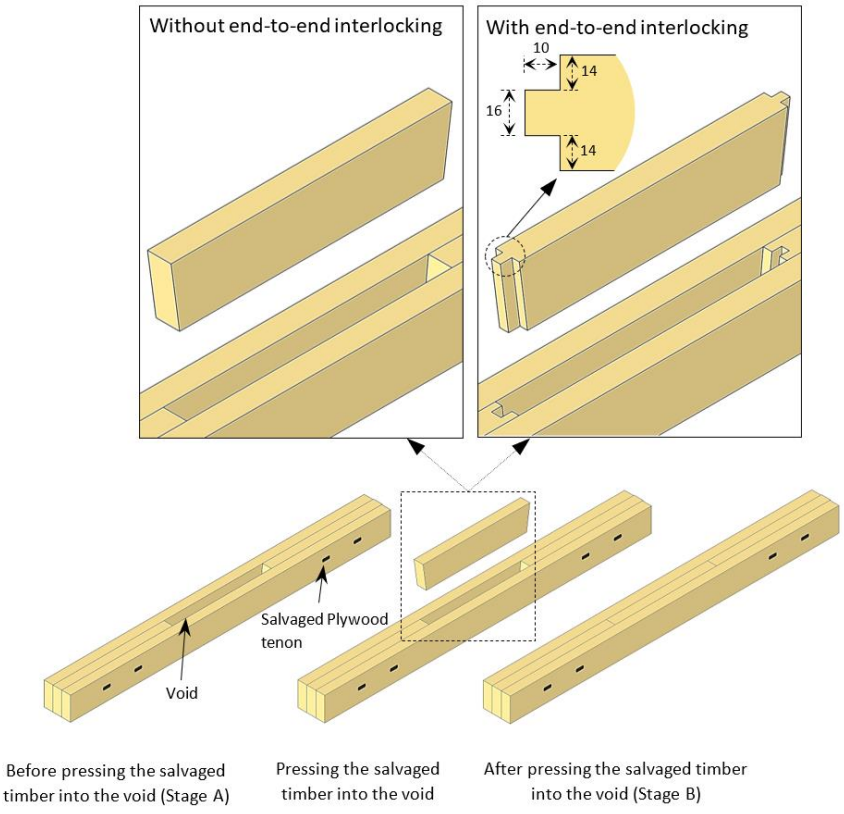

Figure 2. The configurations of the small-scale DLT panels before and after pressing the salvaged timber in the system. Dimensions in mm.

In order to fabricate the small-scale DLT panels, two full-scale timber boards were clamped together with two salvaged timber elements located in the middle. They were then laminated using four salvaged plywood tenons. The holes for the plywood tenons were made using a vertical drill press. As a result of the arrangement of the salvaged timber elements, a void was created in the middle layer (Figure 2). The length of this void was about 2 mm smaller than the length of the salvaged timber element that was supposed to be inserted into the void in the next stage. Afterward, the salvaged timber element was inserted into the void by hammering. As a result of the length difference between the void and the inserted element, the salvaged timber layer was pressed in by the insertion process.

2.2.2. Large-Scale DLT Panels

In total, five large-scale DLT panels were fabricated, which each contained three layers of full-scale sawn timber boards and two layers of salvaged timber elements. The final dimensions of the large-scale DLT panels were $b \times h \times l = 220 \times 117 \times 3500$ mm^3. The cross-sectional area of the plywood tenons was similar to the ones in the small-scale specimens, however, with l = 220 mm. The dimensions of the individual salvaged timber elements are depicted in Figure 3. The inner cross-sections of the salvaged timber elements had been cut at an 88° angle.

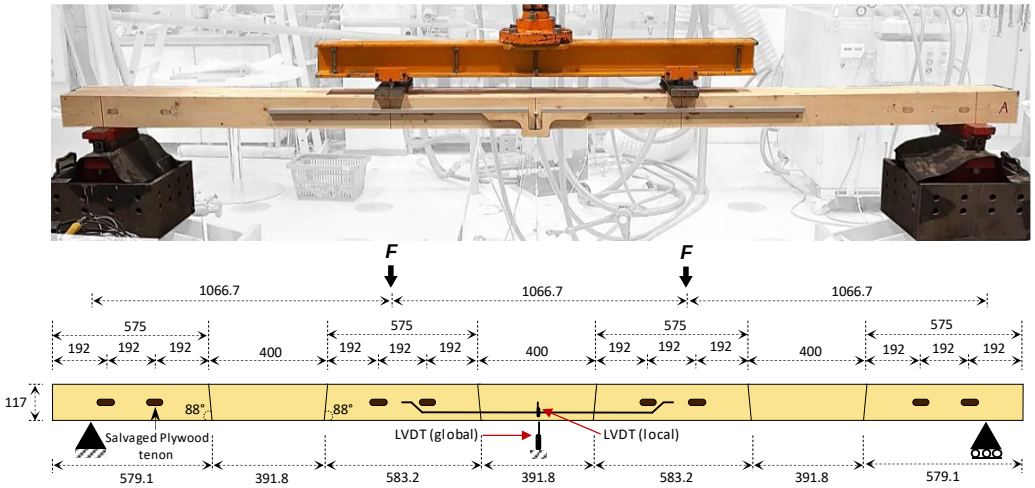

Figure 3. The dimensions of the salvaged timber elements in the large-scale DLT panels and the four-point bending test set-up. Dimensions in mm.

The fabrication process of the large-scale DLT panels is illustrated in Figure 4. Wooden nails (LignoLoc®) made of densified European beech (*F. sylvatica* L.) were used to initially connect the salvaged timber elements to the full-scale timber boards. Two wooden nails were used to connect each salvaged timber element to the adjacent full-scale timber boards. The diameter and the length of the wooden nails were Ø = 4.7 mm and l = 90 mm. The end distance of the wooden nails in relation to the salvaged timber elements was 100 mm. The salvaged timber elements were nailed in such an arrangement that three voids would be created between them in each layer (Figure 4). The length of each void was approximately 2 mm smaller than that of the salvaged timber element that was supposed to be inserted into the void at the final stage of the fabrication. Before inserting the salvaged timber elements into the voids, all the layers were laminated together using eight salvaged plywood tenons with the arrangement and spacing shown in Figure 3. A vertical drill press was used to prepare the holes for the plywood tenons. Six salvaged timber elements were then inserted into the voids of each panel by hammering (Figure 4). As the length of the inserted salvaged timber elements was about 2 mm larger than that of the voids, they were pressed into the system by the insertion process. This way, each layer that contains salvaged timber elements can contribute to the bending performance of the system by resisting compression stress.

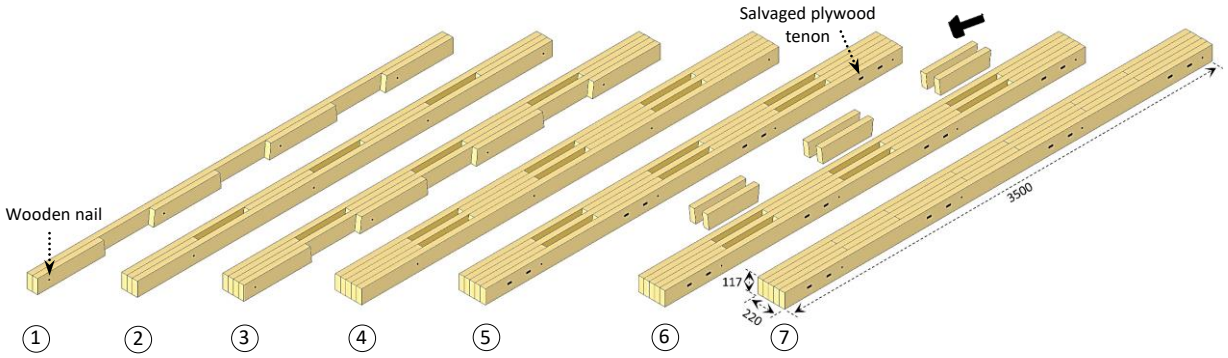

1 Nailing the first row of salvaged timber elements to a new timber board
2 Nailing the second new timber board to the salvaged ones
3 Nailing the second row of salvaged timber elements to the new one
4 Nailing the third new timber board to the salvaged ones
5 Laminating the entire layers using salvaged plywood tenons (Stage A, before inserting the salvaged timber in the system)
6 Placing and hammering the salvaged timber elements into the voids (i.e., inserting the salvaged timber in the system)
7 Final DLT panel (Stage B, after inserting the salvaged timber in the system)

Figure 4. Fabrication steps of the large-scale DLT panels. Dimensions in mm.

2.3. Tests

2.3.1. Overview

The experimental investigation included vibration tests, non-destructive bending tests, and destructive bending tests. Each specimen was investigated two times: before pressing the salvaged timber in the system (the specimen stage is marked as 'Stage A' in Figures 2 and 4) and after pressing the salvaged timber in the system (the specimen stage is marked as 'Stage B' in Figures 2 and 4). The following tests were performed, which are described in more detail in the following subsections:

- Small-scale specimens: Non-destructive three-point bending tests (Stage A and Stage B).
- Large-scale specimens: Non-destructive four-point bending tests (Stage A), destructive four-point bending tests (Stage B), and vibration tests (Stage A and Stage B).

2.3.2. Small-Scale DLT Panels

The global bending stiffness $EI_{m,g}$ of the small-scale DLT panels was investigated non-destructively using a three-point bending test set-up as illustrated in Figure 1. The global mid-span deflection was measured using two LVDTs that were installed on the two full-scale timber boards in the panels. The bending test was load control. A small load level at $0.4 \times F_c$ was selected for the tests in order to ensure that no unexpected damages would occur, where F_c is the load that corresponds to the characteristic value of the bending strength of two layers of full-scale timber boards. In both Stage A and Stage B, the specimens were loaded to $0.4 \times F_c$, unloaded to $0.1 \times F_c$, reloaded to $0.4 \times F_c$, and then fully unloaded.

The $EI_{m,g}$ was calculated from the straight-line portion of the load–deflection curves within the reloading cycle (2nd load cycle) using Equation (1). It should be noted that the actual load-carrying capacity was not measured, as the specimens were needed for subsequent trials afterward, but it is expected that the chosen load range is smaller than given in EN 408 [31].

$$EI_{m,g} = \frac{l^3 \Delta F}{48 \Delta \omega} \ , \tag{1}$$

where $\frac{\Delta F}{\Delta \omega}$ = the slope of the load–deflection curve within 0.1–0.4 $\times$ F_c and l = the span.

2.3.3. Large-Scale DLT Panels

The bending properties of the large-scale DLT panels were measured using a four-point bending test set-up, as shown in Figure 3. During the bending tests, the global mid-span

deflection was measured using three LVDTs that were installed on the bottom surfaces of the three full-scale timber boards in the panels. The local mid-span deflection was also measured using two LVDTs installed on the front and the back of the panels.

For the non-destructive bending tests (Stage A), the specimens were loaded to $0.4 \times F_c$, unloaded to $0.1 \times F_c$, reloaded to $0.4 \times F_c$, and then fully unloaded. After hammering the salvaged timber elements into the voids (Stage B), the bending properties were evaluated as follows: the specimens were loaded to $0.4 \times F_c$, unloaded to $0.1 \times F_c$, and reloaded to $0.4 \times F_c$. The reloading–unloading cycle in the range of 0.1–0.4 $\times F_c$ was repeated ten times in total, and afterward, the specimens were loaded to failure. The test was load control up to $0.7 \times F_c$ and then displacement control thereafter. For Stage B, a higher value of F_c was assumed. Note: for the first specimen tested in Stage B, a lower load range was applied during the test, but it was adjusted for the other specimens.

The $EI_{m,g}$ of the large-scale DLT panels was calculated using the global midspan deflection in accordance with EN 408 [31]. The local bending stiffness $EI_{m,l}$ was calculated using the local midspan deflection. Both $EI_{m,g}$ and $EI_{m,l}$ were obtained from the straight-line portion of the load–deflection curves within the first 'reloading' cycle using the following equations:

$$EI_{m,l} = \frac{al_1^2 \Delta F}{16 \Delta \omega} \ , \tag{2}$$

$$EI_{m,g} = \frac{\left(3al^2 - 4a^3\right) \Delta F}{48 \Delta \omega} \ , \tag{3}$$

where $\frac{\Delta F}{\Delta \omega}$ = the slope of the load–deflection curve within 0.1–0.4 $\times F_c$, a = the distance between the load points and the nearest supports, l = the span, and l_1 = the span of the bar on which the local LVDTs are installed.

During both stages, vibration tests were performed on a simply supported test set-up, as shown in Figure 3. A modal impact hammer, a charge amplifier, an accelerometer, and a dynamic signal analyzer were used for performing the vibration test (Figure 5). The large-scale DLT panels were impacted from the top surface of the middle layer on eleven different points along the span (Figure 5). The spacing between the impact points was 320 mm. Impact points 1 and 11 were located above the supports. The accelerometer was installed on the bottom surface of the middle lamella underneath impact point 5. Each point was impacted three times, and therefore, 33 measurements were collected from each specimen. Data Physics SignalCalc Software was used to record the data.

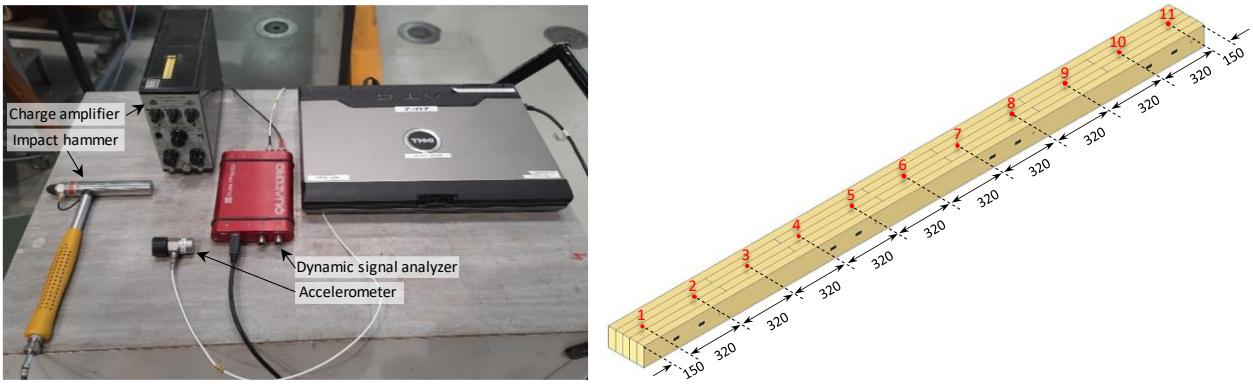

Figure 5. The vibration test instrument (**left**) and the location of the impact points on the large-scale DLT specimens (**right**).

3. Results and Discussion

3.1. Small-Scale DLT Panels

The load–deflection curves of the small-scale DLT panels are shown in Figure 6. It should be noted that the specimens were tested only non-destructively, i.e., they were not

loaded to failure. The calculated $EI_{m,g}$ values of the specimens before and after pressing the salvaged timber elements in the system (i.e., Stage A and Stage B) can be seen in Table 1. A considerable increase of more than 31% in $EI_{m,g}$ was observed after the insertion of the salvaged timber element into the void of the small-scale DLT panels. For both specimen types (with and without end-to-end interlocking), a similar increase in the average bending stiffness was observed, although the variation was higher for the ones without end-to-end interlocking (Table 1). The end-to-end interlocking was not found to make any substantial difference and, therefore, was no longer considered in the subsequent experiments on the large-scale DLT panels.

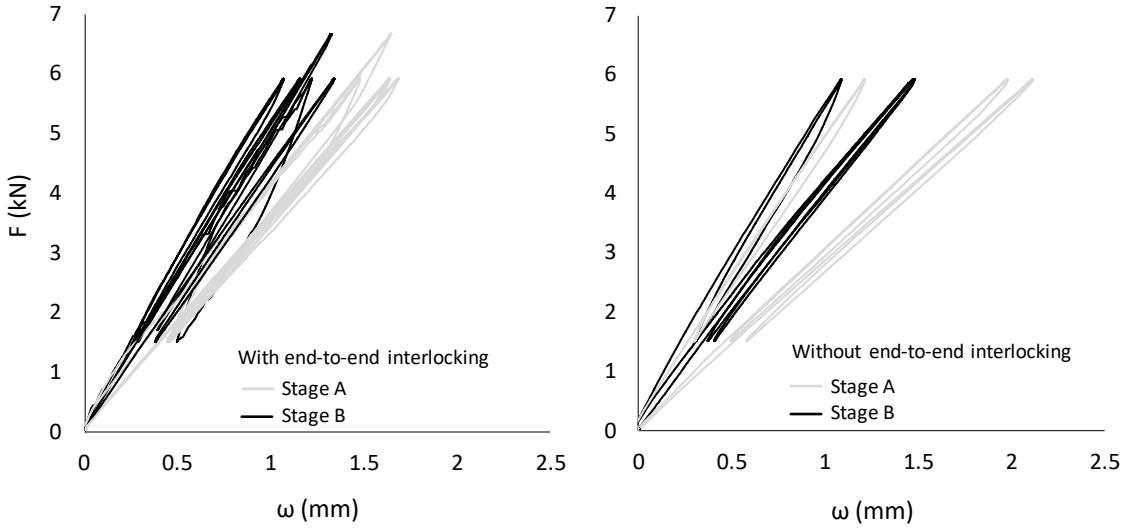

Figure 6. The load–deflection curves of the small-scale DLT panels with and without end-to-end interlocking (the applied load was set slightly higher than intended in the first specimen with end-to-end interlocking).

Table 1. The global bending stiffness $EI_{m,g}$ of the small-scale DLT panels.

Symbol	End-to-End Interlocking	$EI_{m,g}$ (kN.m^2)		Increase (%)
		Stage A	Stage B	
DLT-SY1	Yes	154.8	190.9	23.3
DLT-SY2		132.0	164.3	24.5
DLT-SY3		152.8	196.7	28.7
DLT-SY4		127.8	186.5	45.9
DLT-SY5		131.6	179.9	36.7
Average		139.8	183.7	31.8
COV * (%)		8.3	6.1	
DLT-SN1	No	102.3	144.1	40.9
DLT-SN2		106.0	144.8	36.5
DLT-SN3		171.4	200.0	16.7
Average		126.6	162.9	31.4
COV (%)		25.1	16.1	

* COV = Coefficient of variation.

3.2. Large-Scale DLT Panels

3.2.1. Vibration Characteristics

The results of the vibration tests can be found in Table 2. On average, the first eigenfrequency increased by approximately 6.5% after inserting the salvaged timber elements into the voids. The effect on the damping ratio was inconsistent. The damping ratio decreased in some specimens while it increased in others. It should be noted, however, that the vibration

test, in general, could be quite sensitive to the experimental conditions, see, e.g., [32,33], especially since some specimens had uneven bottom surfaces, which might have affected the support conditions, and consequently, the vibration characteristics.

Table 2. The vibration characteristics of the large-scale DLT panels.

Symbol	f (Hz)		Increase (%)	ζ (%)		Increase or Decrease (%)
	Stage A	Stage B		Stage A	Stage B	
DLT-A	23.8	26.8	12.6	3.7	3.0	−18.9
DLT-B	24.7	25.9	4.9	3.8	3.9	2.6
DLT-C	25.5	25.6	0.4	3.7	5.2	40.5
DLT-D	23.8	26.4	10.9	5.7	1.8	−68.4
DLT-E	26.1	27.1	3.8	5.1	3.4	−33.3
Average	24.8	26.4	6.5	4.4	3.5	−20.5
COV (%)	3.7	2.1		19.1	32.2	

Regardless of the sensitivity issues of the vibration test, it is evident from the obtained results that the (pre-)stresses applied by pressing the salvaged timber elements into the voids affected the first eigenfrequency and damping ratio of the large-scale DLT elements. Whether or not the natural frequency is affected by prestressing has been discussed in some previous studies on other forms of beams made with other types of materials [34,35]. For the interpretation of the results in the study presented here, however, it should be noted that the (pre-)stresses applied here are quite different from the conventional ones.

3.2.2. Load-Carrying Capacity and Failure Modes

Typical load–deflection curves were observed for all large-scale DLT panels, as illustrated in Figure 7. No considerable decrease was detected in the slope of the load–deflection curves up to the failure point. The COV of maximum load-carrying capacity (F_{max}) was relatively small (Table 3), but F_{max} was generally governed by the failure mode of the full-scale timber boards. In order to quantify the effect of pressing the salvaged timber elements in the panels, a comparison to the bending strength of conventional three- and five-layer DLT panels would be needed. However, such tests were not conducted, and due to the low number of test specimens, a qualitative comparison would be any way associated with large uncertainties. However, considering the mean value of the bending stresses $f_{m,\,mean}$ = 56.4 MPa (assuming three continuous layers), a certain effect could be assumed.

The failure of all specimens was characterized by bending failure of the full-scale timber boards, typically initiated around knots in the tension zone (Figure 8). In one specimen (DLT-C), a shear crack in a full-scale timber board near the support was also observed, which indicates that the arrangement of the plywood dowels might need to be optimized. In two other cases (DLT-B and DLT-C), one of the salvaged timber elements split into two parts, which happened near the support. In all specimens, the initial failure always appeared in the full-scale timber boards and not in the salvaged timber elements, as they are not exposed to considerable tension stress due to the absence of end-to-end joining. Therefore, the tension stress is predominantly resisted by the full-scale boards, which leads to failure initiation in the full-scale boards. This indicates that the proposed system is not substantially dependent on the strength properties of the salvaged timber elements. This could be beneficial for a practical application of the system since the strength properties of salvaged timber are typically unknown.

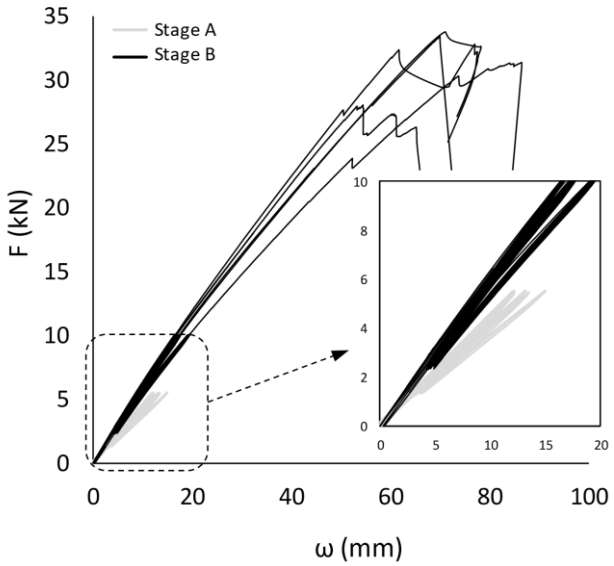

Figure 7. The load–deflection curves of the large-scale DLT panels.

Table 3. The bending properties of the large-scale DLT panels.

Symbol	$EI_{m,l}$ (kN.m^2)		Increase (%)	$EI_{m,g}$ (kN.m^2)		Increase (%)	F_{max} (kN)
	Stage A	Stage B		Stage A	Stage B		Stage B
DLT-A	301.5	399.7	32.6	216.1	306.1	41.6	31.4
DLT-B	338.1	427.2	26.4	243.8	337.6	38.5	33.7
DLT-C	369.8	479.4	29.6	268.7	358.9	33.6	32.8
DLT-D	309.0	490.4	58.7	242.8	345.3	42.2	33.4
DLT-E	374.4	508.8	35.9	267.4	371.3	38.9	28.0
Average	338.6	461.1	36.2	247.8	343.9	38.8	31.9
COV (%)	8.8	8.9		7.8	6.4		6.6

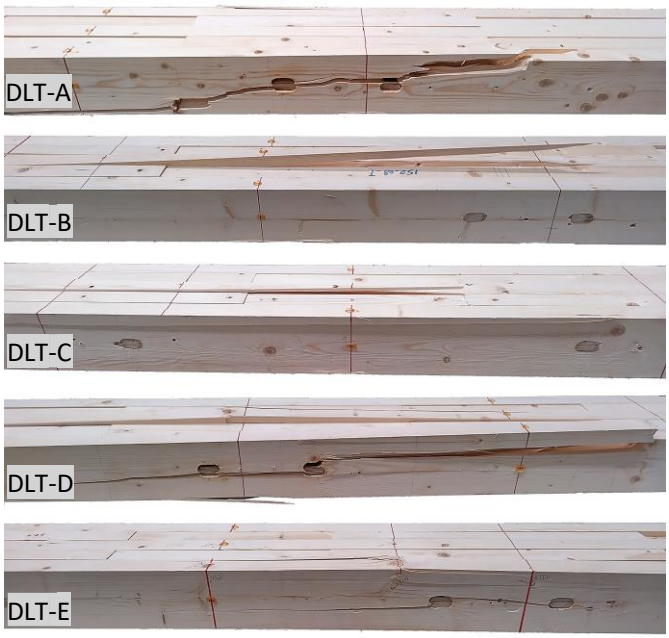

Figure 8. Failure modes of the large-scale DLT panels (view of the bottom surface of the panels).

After the destructive bending tests, three DLT panels (DLT-B, DLT-C, and DLT-D) were deconstructed to evaluate the salvaged plywood tenons. In total, 24 salvaged plywood tenons were inspected. In most of the tenons, no visual deformation was observed. However, in all three DLT panels, one tenon located nearest to the support (the area with the highest shear stresses) had obvious deformations, as shown in Figure 9.

Figure 9. Shear deformations in the salvaged plywood tenons.

3.2.3. Bending Stiffness

The bending stiffness ($EI_{m,g}$ and $EI_{m,l}$) for the two stages was calculated from different load ranges. For Stage A, the load carrying capacity was unknown, and in order to avoid any damage, a small load was applied; therefore, the load range used for the calculations was 1.35–5.42 kN. For Stage B, a larger load range (2.5–10 kN) was used. Nevertheless, considering the load–deflection curves of all the tested specimens (Figure 7), the following conclusions are not much affected by the selected load ranges. Overall, a considerable average increase of approximately 39% for $EI_{m,g}$ and 36.2% for $EI_{m,l}$ was observed after inserting the salvaged timber elements in the panels (Table 3). For both stages and stiffness parameters, the variation was relatively small (COV < 9%).

The increase in the stiffness values may have resulted from the compression resistance provided by the salvaged timber elements. Furthermore, due to the length difference between the inserted timber elements and the voids, some prestressing effect could also be assumed; however, confirmation of this requires further investigations.

3.3. Ease of Fabrication

The ease of fabrication was evaluated during the execution of the study. It was observed that both small-scale and large-scale DLT panels could be fabricated with high accuracy, which is required for ensuring an effective pressed-in system. The hammering of the salvaged plywood tenons was easy; however, it required some effort to hammer the salvaged timber elements into the voids. This was more pronounced for the large-scale DLT panels. Furthermore, in a few cases, some localized cracks were developed parallel to the grain during the insertion process of the salvaged timber elements into the voids. The cracks were assumed to result from uneven impact forces due to hammering on different areas of the salvaged timber elements. Therefore, it might be more effective to insert the salvaged timber elements using a portable hydraulic press instead of hammering.

In terms of time efficiency, the fabrication process of each large-scale DLT panel was completed in about three to four hours (i.e., the sum of hours needed to complete all the fabrication steps mentioned in Figure 4). Additional time was, of course, required to prepare the salvaged plywood tenons and complete the minimal processing of the salvaged timber elements. It should be noted that this time estimate is related to (i) prototyping, (ii) inexperienced staff, and (iii) fabrication processes using conventional woodworking equipment. Therefore, it can be assumed that the fabrication time can be significantly reduced.

4. Conclusions

In the research presented here, a new approach was proposed to reuse short, salvaged timber elements combined with full-scale timber boards in the fabrication of DLT panels without excessive processing or end-to-end joining or gluing. The timber boards were connected with salvaged plywood tenons. In the proposed approach, the salvaged timber elements were pressed in the system in a way that they could resist compression stress under bending loads. The effectiveness of this approach was experimentally evaluated on both small-scale and large-scale DLT panels. The bending stiffness of the small-scale DLT panels, as well as the vibration characteristics, bending properties, and failure modes of the large-scale DLT panels, were experimentally investigated. The following conclusions were drawn:

- The pressed-in salvaged timber elements significantly increased the bending stiffness by more than 31% in the small-scale DLT panels and by 39% in the large-scale DLT panels.
- The first eigenfrequency of the large-scale DLT panels generally increased after pressing the salvaged timber elements in the system, whereas its influence on the damping ratio was inconsistent. The latter could be due to variable support conditions caused by the uneven bottom surface of the panels.
- The load-carrying capacity of the DLT panels was characterized by bending failure of the full-scale timber boards; therefore, the proposed system might not be substantially dependent on the strength properties of the salvaged timber elements. This could be beneficial for a practical application of the system since the strength properties of salvaged timber are typically unknown.

Overall, the results demonstrated a good potential for the proposed approach, which can enable the effective reuse of short, salvaged timber elements in DLT fabrication without the need for excessive processing or gluing. Nevertheless, there are also certain aspects that would require further research and development, some of which are listed as follows:

- Investigation of the long-term performance.
- Analytical investigation of the prestressing effect.
- Development of prediction models for the mechanical properties.
- Optimization of the insertion angle.
- Evaluation of different insertion methods.

Author Contributions: Conceptualization, L.G., M.D. and G.F.; methodology, L.G., M.D. and G.F.; investigation, L.G. and M.D.; formal analysis, L.G., M.D. and G.F.; writing—original draft preparation, M.D.; writing—review and editing, L.G., M.D. and G.F.; visualization, M.D.; supervision, M.D. and G.F.; funding acquisition, G.F. All authors have read and agreed to the published version of the manuscript.

Funding: This research received no external funding.

Data Availability Statement: Some or all data are available from the corresponding author upon reasonable request.

Acknowledgments: The authors are grateful to Joonas Jaaranen (from Aalto University) for his assistance.

Conflicts of Interest: The authors declare no conflict of interest.

References

1. Huuhka, S. Tectonic use of reclaimed timber: Design principles for turning scrap into architecture. *Archit. Res. Finl.* **2018**, *2*, 130–151.
2. Klinge, A.; Roswag-Klinge, E.; Radeljic, L.; Lehmann, M. Strategies for circular, prefab buildings from waste wood. In *IOP Conference Series: Earth and Environmental Science*; IOP Publishing: Bristol, UK, 2019; Volume 225, p. 012052.
3. Derikvand, M.; Hosseinzadeh, S.; Fink, G. Mechanical Properties of Dowel Laminated Timber Beams with Connectors Made of Salvaged Wooden Materials. *J. Archit. Eng.* **2021**, *27*, 04021035. [CrossRef]

4. Niu, Y.; Rasi, K.; Hughes, M.; Halme, M.; Fink, G. Prolonging life cycles of construction materials and combating climate change by cascading: The case of reusing timber in Finland. *Resour. Conserv. Recycl.* **2021**, *170*, 105555. [CrossRef]
5. Ruan, G.; Filz, G.H.; Fink, G. An integrated architectural and structural design concept by using local, salvaged timber. In Proceedings of the IASS Annual Symposium 2020/21 and the 7th International Conference on Spatial Structure: Inspiring the Next Generation, Online, 23–27 August 2021.
6. Azambuja, R.D.R.; Castro, V.G.D.; Trianoski, R.; Iwakiri, S. Recycling wood waste from construction and demolition to produce particleboards. *Maderas. Cienc. Y Tecnol.* **2018**, *20*, 681–690. [CrossRef]
7. Iždinský, J.; Reinprecht, L.; Vidholdová, Z. Particleboards from recycled pallets. *Forests* **2021**, *12*, 1597. [CrossRef]
8. Crews, K. Development of grading rules for re-cycled timber used in structural applications. In *International Council for Research and Innovation in Building and Construction, Working Commission W18–Timber Structures, CIB-W18/40-5-1, Bled, Slovenia*; Universität Karlsruhe: Karlsruhe, Germany, 2007.
9. Crews, K.; MacKenzie, C. Development of grading rules for re-cycled timber used in structural applications. In Proceedings of the World Conference on Timber Engineering (WCTE), Miyazaki, Japan, 2–5 June 2008.
10. Crews, K.; Hayward, D.; MacKenzie, C. *Interim Industry Standard Recycled Timber–Visually Stress Graded Re-cycled Timber for Structural Purposes*; Forest & Wood Products Australia: Melbourne, Australia, 2008; Project No. PN06.1039; ISBN 978-1-920883-35-5.
11. Llana, D.F.; González-Alegre, V.; Portela, M.; Íñiguez-González, G. Cross Laminated Timber (CLT) manufactured with European oak recovered from demolition: Structural properties and non-destructive evaluation. *Constr. Build. Mater.* **2022**, *339*, 127635. [CrossRef]
12. Ma, Y.; Wang, X.; Begel, M.; Dai, Q.; Dickinson, Y.; Xie, X.; Ross, R.J. Flexural and shear performance of CLT panels made from salvaged beetle-killed white spruce. *Constr. Build. Mater.* **2021**, *302*, 124381. [CrossRef]
13. Arbelaez, R.; Schimleck, L.; Sinha, A. Salvaged lumber for Structural Mass Timber Panels: Manufacturing and Testing. *Wood Fiber Sci.* **2020**, *52*, 178–190. Available online: https://wfs.swst.org/index.php/wfs/article/view/2936 (accessed on 20 September 2022). [CrossRef]
14. Rose, C.M.; Bergsagel, D.; Dufresne, T.; Unubreme, E.; Lyu, T.; Duffour, P.; Stegemann, J.A. Cross-laminated secondary timber: Experimental testing and modelling the effect of defects and reduced feedstock properties. *Sustainability* **2018**, *10*, 4118. [CrossRef]
15. Dziurka, D.; Kawalerczyk, J.; Walkiewicz, J.; Derkowski, A.; Mirski, R. The Possibility to Use Pine Timber Pieces with Small Size in the Production of Glulam Beams. *Materials* **2022**, *15*, 3154. [CrossRef]
16. Dziurka, D.; Kuliński, M.; Trociński, A.; Mirski, R. Possibility to Use Short Sawn Timber in the Production of Glued Laminated Beams. *Materials* **2022**, *15*, 2992. [CrossRef] [PubMed]
17. Svensson, S. Duration of load effects of solid wood: A review of methods and models. *Wood Mater. Sci. Eng.* **2009**, *4*, 115–124. [CrossRef]
18. Cavalli, A.; Cibecchini, D.; Togni, M.; Sousa, H.S. A review on the mechanical properties of aged wood and salvaged timber. *Constr. Build. Mater.* **2016**, *114*, 681–687. [CrossRef]
19. Isaksson, T. Modelling the Variability of Bending Strength in Structural Timber-Length and Load Configuration Effects. Ph.D. Dissertation, Lund University, Lund, Sweden, 1999.
20. Fink, G.; Köhler, J. Multiscale variability of stiffness properties of timber boards. In *Applications of Statistics and Probability in Civil Engineering*; Taylor & Francis Group: Abingdon, UK, 2011; pp. 1369–1376.
21. Dietsch, P.; Köhler, J. (Eds.) *Assessment of Timber Structures*; Shaker Verlag: Düren, Germany, 2010; p. 138.
22. Fink, G.; Kohler, J. Quantification of different NDT/SDT methods in respect to estimate the load-bearing capacity. *Constr. Build. Mater.* **2015**, *101*, 1181–1187. [CrossRef]
23. AFTB. Towards Adhesive-Free Timber Buildings (AFTB)-Interreg North-West Europe. 2016. Available online: https://www.nweurope.eu/projects/project-search/towards-adhesive-free-timber-buildings-aftb/ (accessed on 20 June 2022).
24. StructureCraft. Dowel Laminated Timber—The All Wood Panel-Mass Timber Design Guide. 2020. Available online: https://structurecraft.com/blog/dowel-laminated-timber-design-guide-and-profile-handbook (accessed on 20 June 2022).
25. Fink, G.; Ruan, G.; Filz, G.H. Sustainable design concepts for short span, timber-only structures. In Proceedings of the Annual Symposium of the International Association for Shell and Spatial Structures (IASS), Barcelona, Spain, 7 October 2019; Volume 2019, pp. 1–8.
26. Ruan, G.; Filz, G.H.; Fink, G. Shear capacity of timber-to-timber connections using wooden nails. *Wood Mater. Sci. Eng.* **2022**, *17*, 20–29. [CrossRef]
27. Chang, W.S.; Thomson, A.; Harris, R.; Walker, P.; Shanks, J. Development of all-wood connections with plywood flitch plate and oak pegs. *Adv. Struct. Eng.* **2011**, *14*, 123–131. [CrossRef]
28. Daňková, J.; Mec, P.; Šafrata, J. Experimental investigation and performance of timber-concrete composite floor structure with non-metallic connection system. *Eng. Struct.* **2019**, *193*, 207–218. [CrossRef]
29. Derikvand, M.; Fink, G. Deconstructable connector for TCC floors using self-tapping screws. *J. Build. Eng.* **2021**, *42*, 102495. [CrossRef]
30. Derikvand, M.; Fink, G. Bending properties of deconstructable cross-laminated timber-concrete composite floor elements. *Wood Mater. Sci. Eng.* **2022**, *17*, 253–260. [CrossRef]
31. CEN (European Committee for Standardization). *Timber Structures–Structural Timber and Glued Laminated Timber–Determination of some Physical and Mechanical Properties*; EN 408; CEN: Brussels, Belgium, 2010.

32. Pasca, D.P.; Aloisio, A.; Fragiacomo, M.; Tomasi, R. Dynamic characterization of timber floor subassemblies: Sensitivity analysis and modeling issues. *J. Struct. Eng.* **2021**, *147*, 05021008. [CrossRef]
33. Jaaranen, J.; Fink, G. Experimental and numerical investigations of two-way LVL–concrete composite plates with various support conditions. *Eng. Struct.* **2022**, *256*, 114019. [CrossRef]
34. Hamed, E.; Frostig, Y. Natural frequencies of bonded and unbonded prestressed beams–prestress force effects. *J. Sound Vib.* **2006**, *295*, 28–39. [CrossRef]
35. Aloisio, A. Aspects of vibration-based methods for the prestressing estimate in concrete beams with internal bonded or unbonded tendons. *Infrastructures* **2021**, *6*, 83. [CrossRef]